analytical chemistry

Letter

pubs.acs.org/ac

Biocomposite Based on Reduced Graphene Oxide Film Modified with Phenothiazone and Flavin Adenine Dinucleotide-Dependent Glucose Dehydrogenase for Glucose Sensing and Biofuel Cell Applications

Yehonatan Ravenna,[†] Lin Xia,[†] Jenny Gun,[‡] Alexey A. Mikhaylov,[‡] Alexander G. Medvedev,[‡] Ovadia Lev,*[,‡] and Lital Alfonta*[,†]

[†]Department of Life Sciences and the Ilse Katz Institute for Nanoscale Science and Technology, Ben-Gurion University of the Negev, P.O. Box 653, Beer-Sheva 84105, Israel

[‡]The Casali Institute, The Institute of Chemistry, and The Harvey M. Krueger Family Center for Nanoscience and Nanotechnology, The Hebrew University of Jerusalem, Jerusalem 91904, Israel

Supporting Information

ABSTRACT: A novel composite material for the encapsulation of redox enzymes was prepared. Reduced graphene oxide film with adsorbed phenothiazone was used as a highly efficient composite for electron transfer between flavin adenine dinucleotide (FAD)-dependent glucose dehydrogenase and electrodes. Measured redox potential for glucose oxidation was lower than 0 V vs Ag/AgCl electrode. The fabricated biosensor showed high sensitivity of 42 mA M^{-1} cm^{-2}, a linear range of glucose detection of 0.5−12 mM, and good reproducibility and stability as well as high selectivity for different interfering compounds. In a semibiofuel cell configuration, the hybrid film generated high power output of 345 μW cm^{-2}. These results demonstrate a promising potential for this composition in various bioelectronic applications.

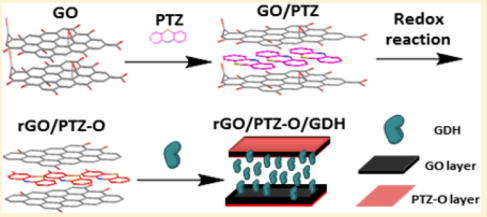

In the past decade, graphene has emerged as a very promising substrate for both enzymatic[1] and nonenzymatic sensing.[2] Its oxidized form, graphene oxide (GO), which represents a new class of two-dimensional nanostructure, has attracted a great deal of attention due to its unique properties and potential applications in capacitors,[3] batteries,[4] solar cell electrolytes,[5] sensors,[6] electronic devices,[7,8] cell imaging, drug delivery,[9] and biofuel cells.[10] First prepared almost 150 years ago, GO has emerged as a precursor offering the potential of a cost-effective, large-scale production of graphene-based materials.[11,12] Graphene oxide is an atomically thin sheet of graphite, covalently decorated with oxygen-containing functional groups, either on the middle of the graphene plane or at the edges, so that it contains a mixture of sp^2 and sp^3 hybridized carbon atoms.[13] The use of GO in electrically active materials and devices is still limited by the high electrical resistance associated with the presence of carboxyl, hydroxyl, carbonyl, or epoxy groups in GO sheets. However, the presence of oxygen-containing functional groups provides potential advantages to GO in numerous applications. For example, Liu et al. covalently attached the amine groups of glucose oxidase to carboxylic acid residues on GO to achieve covalent immobilization of an enzyme to GO.[14] In addition, the oxygen groups provide high solubility to GO and enable it to form a hydrogel, thus to encapsulate microorganisms and enzymes. GO has demonstrated a promising biocompatibility where even live cells could be encapsulated and proliferate; however, it suffers from limited conductivity.[15]

The reduction of graphene oxide to its reduced form (rGO) has recently gained considerable attention since it partially restores the remarkable physical and electrical properties of graphenes, while still benefiting from the presence of oxygen-functional groups. Reduction can be achieved by thermal, electrochemical,[16] chemical,[17] and bioelectrocatalytic treatments.[15] rGO is more conductive than GO, while still maintaining its biocompatible properties when used for enzyme-based sensing.[6] We have reasoned that we may be able to improve the performance of a biosensor using rGO by introducing redox mediators into GO and then reduce it to rGO in the presence of an enzyme of choice. Hence, we have chosen to use phenothiazine (PTZ). PTZ and its derivatives (including methylene blue,[18] phenazine,[19] thionine,[20] azure B,[21] and toluidine blue O[22]) are widely used as electron mediators for bioelectronic applications due to their low formal redox potentials at pH 7, which ranges between −300 mV for methylene blue to 240 mV for toluidine blue O vs Ag/AgCl reference electrode. Sekretaryova et al., for example, have recently used PTZ immobilized in siloxane sol−gel for mediation of electron transfer between oxidases and electrodes.[23] When we used PTZ in our GO matrix, we could solubilize the PTZ in the presence of GO platelets; however, we noticed that its electrochemical behavior in GO had been changed considerably. After a thorough chemical character-

Received: August 2, 2015
Accepted: September 3, 2015

DOI: 10.1021/acs.analchem.5b02949
Anal. Chem. XXXX, XXX, XXX−XXX

ization (Supporting Information), we concluded that it was not PTZ in our matrix, but rather an irreversibly oxidized form of PTZ, namely, 3*H*-phenothiazine-3-one (phenothiazone, PTZ-O).[24,25] The PTZ-O electrochemical behavior proved promising as a redox mediator suitable for anodic processes with reversible electrochemical characteristics and a middle point potential of ca. −70 mV vs Ag/AgCl, and most importantly in contrast with PTZ, PTZ-O is highly soluble. To the best of our knowledge, PTZ-O has not been used before for biosensing as a mediator nor has it been combined with rGO. Hence, as a proof of concept, we have set out to use this unique combination of rGO and PTZ-O for an enzymatic glucose sensing. Among the different redox enzymes used in biosensing, glucose oxidase (GOx) is widely used as a biocatalyst in glucose sensing due to its high thermostability and good catalytic ability to oxidize glucose. However, since the natural electron acceptor of GOx is dioxygen (O_2), it competes with the mediator over the electrons, thus interfering with biosensor performance.[26,27] In contrast, glucose dehydrogenase (GDH), which does not utilize O_2 as an electron acceptor, is a good candidate for oxygen-independent glucose sensing. Moreover, GDH does not produce hydrogen peroxide. Hydrogen peroxide inhibits laccase and bilirubin oxidase activity[28,29] when used as cathodic enzymes in biofuel-cells. Flavin adenine dinucleotide-dependent GDH (FAD-GDH E.C. 1.1.5.9) shows high thermostability and good glucose specificity and does not require an exogenous addition of a cofactor, as the FAD cofactor is tightly bound to the enzyme.[30] Herein, we report the preparation, characterization, and the performance of a glassy carbon electrode (GCE) coated with rGO/PTZ-O/GDH film used for biosensing as well as for biofuel cell applications.

Electrochemical properties of the new composite material of rGO/PTZ-O/GCE have been studied by cyclic voltammetry (CV). Figure 1A shows a CV of rGO modified with PTZ-O (rGO/PTZ-O) (a) and a solution with the soluble fraction of mostly insoluble PTZ (b) using a glassy carbon electrode (GCE) as the working electrode. The middle point potential ($E_{1/2}$) of PTZ in an aqueous solution was calculated as the mean of the anodic peak (E_{pa}) and cathodic peak (E_{pc}) to be 280 mV vs Ag/AgCl. Upon adsorption of PTZ on GO platelets, PTZ was oxidized to PTZ-O by GO, which in turn was partially reduced to rGO. In this process, PTZ-O accumulated while PTZ has diminished (Figure 1A, curve a). For the purified PTZ-O extracted from the PTZ modified rGO matrix, a reversible electrochemical behavior was observed with a middle point potential of $E_{1/2}$ = −70 mV (Figure 1B) and a peak-to-peak separation of ca. ΔE = 60 mV which corresponds to a complete reversible behavior of a one electron redox process. In order to identify the oxidized PTZ, purified PTZ-O was characterized by H NMR, C NMR, and high resolution LC-MS analysis (Figures S1−S3). We have collected an LC-MS fraction that corresponded to a mass of 214.033 Da. Cyclic voltammetry was performed on the collected fraction and indeed confirmed that the molecule with a mass of 214.13 Da is the source of the newly generated redox peak. Figure 2 shows

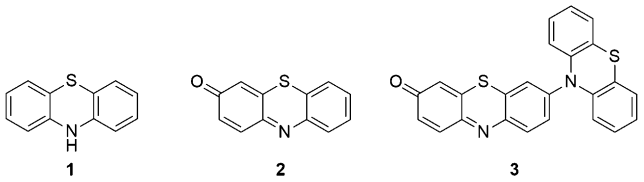

Figure 2. Chemical structure of (**1**) phenothiazine (PTZ), (**2**) 3*H*-phenothiazine-3-one (PTZ-O), and (**3**) a dimer of PTZ and PTZ-O.

the structure of PTZ (**1**) and PTZ-O (**2**) as was determined by our MS and NMR analyses. LC-MS analysis has also shown that another oxidized species exists in the GO upon graphene reduction and PTZ oxidation, a dimer shown in Figure 2 (**3**), which is a combination of PTZ and PTZ-O. This combination was further verified by CV, and it has shown similar voltammograms as is seen for both PTZ and PTZ-O when put together in a solution with one peak at 280 mV and one peak at −70 mV. The dimer (**3**), however, is present in smaller quantities in the GO matrix, and the dominant species is PTZ-O (**2**). In Figure 1B, a reversible voltammogram of pure PTZ-O can be observed. PTZ-O adsorbed in rGO shows reversible electrochemical voltammograms with a surface confined process dependence as indicated by the measurements shown in Figure 1C (inset) with a linear dependence of anodic and cathodic peak currents with scan rate. CVs remain essentially unchanged on consecutive potential scan cycles indicating that rGO/PTZ-O modified electrode remains stable over time and polarization.

In order to determine the number of electrons transferred per molecule, we tested the voltammetric response of the modified electrode under pH values varying between pH 4.0 to 8.0 (Figure 1D). The formal potential is pH dependent with a negative shift with increasing pH (inset of Figure 1D).

Results were plotted as $E_{1/2}$ vs pH; slope was calculated to be 52.9 mV/pH, which is close to the Nernstian value of 59.2 mV/pH in the modified form of Nernst's equation[31] which represents a 1 electron transfer process. The electron transfer coefficient (α) can be calculated according to Laviron's equation.[32] In this case, the anodic peak potential changed linearly vs. the natural logarithm of scan rate (ν) in the range of 60 to 450 mV/s and α can be obtained from the slope of the curve (Figure S4A). An electron transfer coefficient of 0.37 was estimated for the reversible redox reaction, indicating a good symmetry between the forward and reverse electron transfer

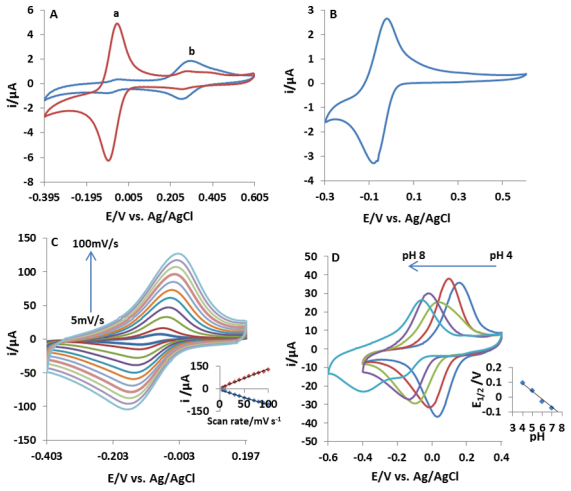

Figure 1. Cyclic voltammograms (CVs) of GC electrodes. (A) (a) rGO/PTZ after oxidation and (b) PTZ in solution; (B) CV of pure PTZ-O extracted from rGO; (C) CVs at different scan rates. Inset: scan rate-dependent peak currents of rGO/PTZ-O/GCE; (D) CVs of rGO/PTZ-O/GCE pH dependence; inset: middle point potentials vs pH.

DOI: 10.1021/acs.analchem.5b02949
Anal. Chem. XXXX, XXX, XXX−XXX

step and an apparent electron transfer rate constant of k_{app}= 0.535 s^{-1}. Average surface concentration (Γ) of the electroactive compound (PTZ-O) in rGO on the surface of a glassy carbon electrode was extracted from a Laviron's plot (Figure S4B). Using Laviron's theory,[32] the value of Γ was calculated to be 2 × 10^{-8} mol/cm^2. When other electroactive compounds immobilized on GCE were compared, we could conclude that a high number of PTZ-O molecules are successfully immobilized and available in this system.[33,34] This high surface concentration can be attributed to the high surface area of GO nanoplatelets and an efficient interaction between PTZ-O and rGO.

In order to further verify our proposed model for GO reduction and PTZ oxidation, we have performed Raman spectroscopy measurements of the relative D and G bands of graphene. The G band (around 1580 cm^{-1}) is common to all sp^2 carbon atoms, whereas the D band is attributed to sp^3 atoms and the disordered structure of graphene. Indeed, the small changes in the D/G bands ratio cannot provide a clear indication for the reduction of the graphene oxide by PTZ (Figure S5A), in agreement with Yang et al.[35]

Hence, we wanted to further verify the reduction by XPS. Figure S5B shows the XPS C1S binding energy spectra of GO samples before and after reduction by PTZ; the quantity of oxygenated carbon atoms on the graphene has substantially decreased after exposure to PTZ.

Enzymes can be immobilized efficiently by a simple and nondestructive entrapment in GO hydrogels. On the basis of the flexibility of GO hydrogel and robustness of PTZ-O as a reversible redox compound, a simple and facile method was developed to create a film-like biocomposite on the surface of glassy carbon electrode. In this way, we fabricated a film modified electrode, comprising an enzyme, mediator, and rGO. The film production was based on published reports by Yulaev et al.[36] To investigate the catalytic performance of rGO/PTZ-O biocomposite towards glucose oxidation, FAD-GDH was immobilized within the composite to serve as a biocatalyst. FAD-GDH was expressed in *E. coli* and was purified according to Inose et al.[37] Bacterially expressed enzymes lack post translational modifications such as glycosylations;[38] hence, less interference with electron transfer between the enzyme active site and any electron acceptor is expected. Faradaic impedance spectroscopy measurements of rGO/PTZ-O/GDH film were used to extract conductivity values of the film before and after electrochemical reduction yielding values of 20 and 420 mS/cm^2, respectively (Supporting Information). Figure 3A shows the bioelectrocatalytic current evolved using rGO/PTZ-O/GDH/GCE in the presence of varying concentrations of glucose. The enzymatic oxidation of glucose is visible as an anodic current with an onset potential of −0.25 V and is related to the oxidation of FAD mediated by PTZ-O immobilized on rGO film. The inset of Figure 3A shows a linear relationship between glucose concentration and anodic current. Hence, we tested the amperometric response of rGO/PTZ-O/GDH modified glassy carbon electrode to increasing glucose concentrations. Electrochemical reduction was performed on the rGO film by applying a constant potential of −0.85 V for 200 s, resulting in an increase in capacitance of the system while still keeping the enzyme activity intact. Figure 3B shows the amperometric response of a biosensor for standard additions of 1, 2, and 5 mM glucose at an applied potential of 0.1 V. The dynamic range of the rGO/PTZ-O/GDH modified GC electrode after the additional electrochemical reduction is

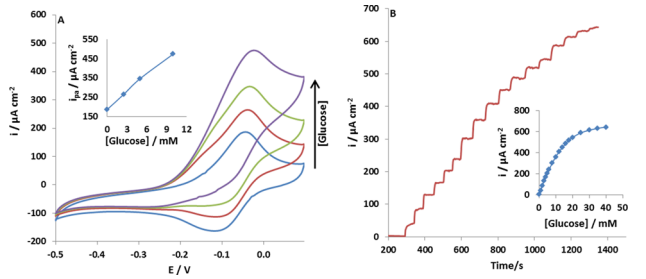

Figure 3. (A) CVs of rGO/PTZ-O/GDH modified glassy carbon electrode in the absence of glucose (blue line) and in the presence of elevated glucose concentrations (red, green, and purple lines); inset: calibration curve for the peak oxidation current upon addition of different glucose concentrations. (B) Chronoamperometric response of rGO/PTZ-O/GDH modified glassy carbon electrode for the successive additions of glucose; inset: calibration curve for the steady state current upon addition of different glucose concentrations.

between 0.5 and 40 mM, and the linear range is 0.5−12 mM. Sensitivity was calculated from the slope of the linear part of the calibration curve (Figure 3B, inset) and found to be ca. 42 mA $M^{-1}cm^{-2}$, that is among the highest reported values compared to other reported glucose biosensors. The apparent Michaelis−Menten (K_m^{app}) constant could be derived using the electrochemical Lineweaver−Burk eq (Figure S9). The K_m^{app} value of the enzyme on the modified electrode was calculated to be 2.6 mM compared to a reported K_m of 10 mM for NAD-GDH[39] and 17 mM for a free FAD-GDH.[40] This value is fairly low compared to other GDH biosensors,[41,42] indicating improved affinity to glucose when entrapped in rGO/PTZ-O film. Additional characteristics of biosensor performance such as reproducibility, standard deviation of sensor, and selectivity are reported in detail in the Supporting Information.

Next, we tested the rGO/PTZ-O/GDH modified GC electrode performance as an anode in a biofuel cell. To eliminate limitations from the cathode, the cathode was controlled by a potentiostat and was biased continuously to 400 mV. Figure 4 shows the polarization curve and power outputs of a biofuel cell constructed from rGO/PTZ-O/GDH modified GCE.

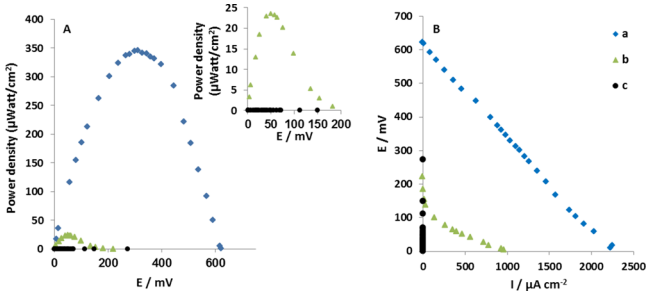

Figure 4. Power output (A) and polarization curves (B) of (a) rGO/PTZ-O/GDH; (b) rGO/PTZ-O/GOx; (c) rGO/PTZ-O; modified electrodes; inset: magnified curves (b) and (c) on a lower scale. Cathode was electrochemically biased to 400 mV.

An electrochemical reduction procedure was applied to further increase GO capacitance to perform better in a biofuel cell. From Figure 4A, it can be seen that power output generated by GDH encapsulated in rGO/PTZ-O matrix is as high as 345 μW/cm^2 which is comparable to previously reported GDH based biofuel cells,[29,43] although one should

DOI: 10.1021/acs.analchem.5b02949
Anal. Chem. XXXX, XXX, XXX−XXX

note that what we describe is a semibiofuel cell and a bacterial FAD-GDH (i.e., without posttranslational modifications); hence, it is not a comparison of the exact same systems. This performance can be attributed to the robustness of rGO, GDH, and PTZ-O, efficient electron transfer between bacterial GDH and rGO/PTZ-O matrix, and an increase in conductivity of the rGO by the further electrochemical reduction and thus an increase in electron transfer rates and efficiency. As control experiments, we entrapped glucose oxidase (GOx) instead of GDH in the rGO/PTZ-O matrix or used no enzyme at all. rGO/PTZ-O/GOx bioanode produced a power output of 23.6 $\mu W/cm^2$, a decrease of more than 90% in power compared to the 345 $\mu W/cm^2$ produced by the rGO/PTZ-O/GDH bioanode. This can be an indication of the efficient utilization of PTZ-O as a mediator by GDH. The fill factor (f) of the biofuel cell using rGO/PTZ-O/GDH as a bioanode was calculated according to eq S1 using data from the polarization curve shown in Figure 4B and found to be ca. 25%. The low fill factor indicates a significant deviation from the optimal rectangular-shaped polarization curve. Nevertheless, from comparison of polarization curves shown in Figure 4B, it can be clearly seen that GDH shows a superior performance compared to GOx when encapsulated in rGO/PTZ-O matrix.

We have introduced a novel biocomposite made of rGO and PTZ-O using a facile procedure, which mediates an efficient and robust electron transfer between the FAD cofactor of GDH and an electrode. The high sensitivity, stability, and selectivity render the system promising for glucose biosensing. The ability of rGO to encapsulate enzymes and form a film contributes to its appeal in future biosensing applications. Moreover, the low operating potential of the system as well as good communication of GDH with the mediator enables the system to serve as an efficient bioanode for the electrocatalytic oxidation of glucose in a biofuel cell. The robustness of modified graphene oxide with PTZ-O and the flexibility of the hydrogel to entrap biomolecules demonstrate its great potential in bioelectronic systems.

■ ASSOCIATED CONTENT

Supporting Information

The Supporting Information is available free of charge on the ACS Publications website at DOI: 10.1021/acs.analchem.5b02949.

Detailed experimental procedures, chemical characterization of PTZ-O, statistical data, calibration curves, control experiments, and additional electrochemical characterization (PDF)

■ AUTHOR INFORMATION

Corresponding Authors

*E-mail: ovadia@vms.huji.ac.il. Fax: +972-2-6586155. Tel: +972-2-6584191.

*E-mail: alfontal@bgu.ac.il. Fax: +972-8-6479576. Tel: +972-8-6479066.

Notes

The authors declare no competing financial interest.

■ ACKNOWLEDGMENTS

Research was supported by an Israel Science Foundation (ISF) Program (232/13), L.A. and O.L., as well as by European Research Council (ERC) Grant Agreement No. 260647 (L.A.), Ministry of Science Infrastructure Research Program in Analytical Chemistry (O.L.), PBC program for fellowships for outstanding postdoctoral researchers from China and India (L.X.), and Golda Meir and Vallazzi-Pikovski Posdoctoral Fellowships (A.G.M and A.A.M). We gratefully acknowledge Dr. Josep Rayo for NMR analyses. Y.R. is supported by a fellowship from the Department of Biotechnology Engineering, Ben-Gurion University of the Negev.

■ REFERENCES

(1) Kuila, T.; Bose, S.; Khanra, P.; Mishra, A. K.; Kim, N. H.; Lee, J. H. *Biosens. Bioelectron.* **2011**, *26*, 4637−4648.

(2) Hill, E. W.; Vijayaragahvan, A.; Novoselov, K. *IEEE Sens. J.* **2011**, *11*, 3161−3170.

(3) Stoller, M. D.; Park, S.; Zhu, Y.; An, J.; Ruoff, R. S. *Nano Lett.* **2008**, *8*, 3498−3502.

(4) Yu, D. Y. W.; Prikhodchenko, P. V.; Mason, C. W.; Batabyal, S. K.; Gun, J.; Sladkevich, S.; Medvedev, A. G.; Lev, O. *Nat. Commun.* **2013**, *4*, 2922.

(5) Gun, J.; Kulkarni, S. A.; Xiu, W.; Batabyal, S. K.; Sladkevich, S.; Prikhodchenko, P. V.; Gutkin, V.; Lev, O. *Electrochem. Commun.* **2012**, *19*, 108−110.

(6) Zhou, M.; Zhai, Y.; Dong, S. *Anal. Chem.* **2009**, *81*, 5603−5613.

(7) Gilje, S.; Han, S.; Wang, M.; Wang, K. L.; Kaner, R. B. *Nano Lett.* **2007**, *7*, 3394−3398.

(8) Li, B.; Cao, X.; Ong, H. G.; Cheah, J. W.; Zhou, X.; Yin, Z.; Li, H.; Wang, J.; Boey, F.; Huang, W.; Zhang, H. *Adv. Mater.* **2010**, *22*, 3058−3061.

(9) Sun, X.; Liu, Z.; Welsher, K.; Robinson, J. T.; Goodwin, A.; Zaric, S.; Dai, H. *Nano Res.* **2008**, *1*, 203−212.

(10) Palanisamy, S.; et al. *Int. J. Electrochem. Sci.* **2012**, *7*, 11477−11487.

(11) Hernandez, Y.; Nicolosi, V.; Lotya, M.; Blighe, F. M.; Sun, Z.; De, S.; McGovern, I. T.; et al. *Nat. Nanotechnol.* **2008**, *3*, 563−568.

(12) Murugan, A. V.; Muraliganth, T.; Manthiram, A. *Chem. Mater.* **2009**, *21*, 5004−5006.

(13) Loh, K. P.; Bao, Q.; Eda, G.; Chhowalla, M. *Nat. Chem.* **2010**, *2*, 1015−1024.

(14) Liu, Y.; Yu, D.; Zeng, C.; Miao, Z.; Dai, L. *Langmuir* **2010**, *26*, 6158−6160.

(15) Bahartan, K.; Gun, J.; Sladkevich, S.; Prikhodchenko, P. V.; Lev, O.; Alfonta, L. *Chem. Commun.* **2012**, *48*, 11957−11959.

(16) Shao, Y.; Wang, J.; Engelhard, M.; Wang, C.; Lin, Y. *J. Mater. Chem.* **2010**, *20*, 743−748.

(17) Chen, W.; Yan, L.; Bangal, P. R. *J. Phys. Chem. C* **2010**, *114*, 19885−19890.

(18) Xu, J.-Z.; Zhu, J.-J.; Wu, Q.; Hu, Z.; Chen, H.-Y. *Electroanalysis* **2003**, *15*, 219−224.

(19) Pauliukaite, R.; Ghica, M. E.; Barsan, M. M.; Brett, C. M. a. *Anal. Lett.* **2010**, *43*, 1588−1608.

(20) Xu, J.-J.; Zhou, D.-M.; Chen, H.-Y. *Electroanalysis* **1998**, *10*, 713−716.

(21) Shan, D.; Mousty, C.; Cosnier, S.; Mu, S. *Electroanalysis* **2003**, *15*, 1506−1512.

(22) Boguslavsky, L. I.; Geng, L.; Kovalev, I. P.; Sahni, S. K.; Xu, Z.; Skotheim, T. a.; Laurinavicius, V.; Persson, B.; Gorton, L. *Biosens. Bioelectron.* **1995**, *10*, 693−704.

(23) Sekretaryova, A. N.; Vagin, M. Y.; Beni, V.; Turner, A. P. F.; Karyakin, A. a. *Biosens. Bioelectron.* **2014**, *53*, 275−282.

(24) Underberg, W. J. M. *J. Pharm. Sci.* **1978**, *67*, 1128−1131.

(25) Roseboom, H.; Perrin, J. H. *J. Pharm. Sci.* **1977**, *66*, 1392−1395.

(26) Shan, C.; Yang, H.; Song, J.; Han, D.; Ivaska, A.; Niu, L. *Anal. Chem.* **2009**, *81*, 2378−2382.

(27) Gregg, B. A.; Heller, A. *Anal. Chem.* **1990**, *62*, 258−263.

(28) Scodeller, P.; Carballo, R.; Szamocki, R.; Levin, L.; Forchiassin, F.; Calvo, E. J. *J. Am. Chem. Soc.* **2010**, *132*, 11132−11140.

(29) Milton, R. D.; Giroud, F.; Thumser, A. E.; Minteer, S. D.; Slade, R. C. T. *Phys. Chem. Chem. Phys.* **2013**, *15*, 19371−19379.

DOI: 10.1021/acs.analchem.5b02949
Anal. Chem. XXXX, XXX, XXX−XXX

(30) Tsujimura, S.; Kojima, S.; Kano, K.; Ikeda, T.; Sato, M.; Sanada, H.; Omura, H. *Biosci., Biotechnol., Biochem.* **2006**, *70*, 654−659.
(31) Delahay, P.; Pourbaix, M.; Van Rysselberghe, P. *J. Chem. Educ.* **1950**, *27*, 683.
(32) Laviron, E. J. *J. Electroanal. Chem. Interfacial Electrochem.* **1979**, *101*, 19−28.
(33) Hong, J.; Zhao, Y.-X.; Xiao, B.-L.; Moosavi-Movahedi, A. A.; Ghourchian, H.; Sheibani, N. *Sensors* **2013**, *13*, 8595−8611.
(34) Lin, K.-C.; Jian, X.-C.; Chen, S.-M. *Int. J. Electrochem. Sci.* **2011**, *6*, 2264−2283.
(35) Yang, D.; Velamakanni, A.; Bozoklu, G.; Park, S.; Stoller, M.; Piner, R. D.; Stankovich, S.; Jung, I.; Field, D. A.; Ventrice, C. A., Jr.; Ruoff, R. S. *Carbon* **2009**, *47*, 145−152.
(36) Yulaev, A.; Lipatov, A.; Sinitskii, A.; Kolmakov, A. *Microsc. Microanal.* **2014**, *20*, 1798−1799.
(37) Inose, K.; Fujikawa, M.; Yamazaki, T.; Kojima, K.; Sode, K. *Biochim. Biophys. Acta, Proteins Proteomics* **2003**, *1645*, 133−138.
(38) Tsuya, T.; Ferri, S.; Fujikawa, M.; Yamaoka, H.; Sode, K. *J. Biotechnol.* **2006**, *123*, 127−136.
(39) Smith, L. D.; Budgen, N.; Bungard, S. J.; Danson, M. J.; Hough, D. W. *Biochem. J.* **1989**, *261*, 973−977.
(40) Yamaoka, H.; Yamashita, Y.; Ferri, S.; Sode, K. *Biotechnol. Lett.* **2008**, *30*, 1967−1972.
(41) Dokter, P.; Frank, J.; Duine, J. A. *Biochem. J.* **1986**, *239*, 163−167.
(42) Zafar, M. N.; Beden, N.; Leech, D.; Sygmund, C.; Ludwig, R.; Gorton, L. *Anal. Bioanal. Chem.* **2012**, *402*, 2069−2077.
(43) Hou, C.; Fan, S.; Lang, Q.; Liu, A. *Anal. Chem.* **2015**, *87*, 3382−3387.

DOI: 10.1021/acs.analchem.5b02949
Anal. Chem. XXXX, XXX, XXX−XXX